Evidence for massive and recurrent toxic blooms of *Alexandrium catenella* in the Alaskan Arctic

Donald M. Anderson[a,1], Evangeline Fachon[a], Robert S. Pickart[b], Peigen Lin[b], Alexis D. Fischer[a], Mindy L. Richlen[a], Victoria Uva[a], Michael L. Brosnahan[a], Leah McRaven[b], Frank Bahr[b], Kathi Lefebvre[c], Jacqueline M. Grebmeier[d], Seth L. Danielson[e], Yihua Lyu[f], and Yuri Fukai[g]

[a]Biology Department, Woods Hole Oceanographic Institution, Woods Hole, MA 02543; [b]Physical Oceanography Department, Woods Hole Oceanographic Institution, Woods Hole, MA 02543; [c]Environmental and Fisheries Sciences Division, Northwest Fisheries Science Center, NOAA to National Oceanic and Atmospheric Administration, National Marine Fisheries Service, Seattle, WA 98112; [d] Chesapeake Biological Laboratory, University of Maryland Center for Environmental Sciences, Solomons, MD 20688; [e]College of Fisheries and Ocean Sciences, University of Alaska Fairbanks, Fairbanks, AK 99775; [f]South China Sea Environmental Monitoring Center, State Oceanic Administration, Guangzhou 510300, People's Republic of China; and [g]Graduate School of Environmental Science, Hokkaido University, Sapporo, Hokkaido, 060-0810, Japan

Edited by David M. Karl, University of Hawaii at Manoa, Honolulu, HI, and approved August 19, 2021 (received for review April 22, 2021)

Among the organisms that spread into and flourish in Arctic waters with rising temperatures and sea ice loss are toxic algae, a group of harmful algal bloom species that produce potent biotoxins. *Alexandrium catenella*, a cyst-forming dinoflagellate that causes paralytic shellfish poisoning worldwide, has been a significant threat to human health in southeastern Alaska for centuries. It is known to be transported into Arctic regions in waters transiting northward through the Bering Strait, yet there is little recognition of this organism as a human health concern north of the Strait. Here, we describe an exceptionally large *A. catenella* benthic cyst bed and hydrographic conditions across the Chukchi Sea that support germination and development of recurrent, locally originating and self-seeding blooms. Two prominent cyst accumulation zones result from deposition promoted by weak circulation. Cyst concentrations are among the highest reported globally for this species, and the cyst bed is at least 6× larger in area than any other. These extraordinary accumulations are attributed to repeated inputs from advected southern blooms and to localized cyst formation and deposition. Over the past two decades, warming has likely increased the magnitude of the germination flux twofold and advanced the timing of cell inoculation into the euphotic zone by 20 d. Conditions are also now favorable for bloom development in surface waters. The region is poised to support annually recurrent *A. catenella* blooms that are massive in scale, posing a significant and worrisome threat to public and ecosystem health in Alaskan Arctic communities where economies are subsistence based.

harmful algal bloom | HAB | Alexandrium | Alaskan Arctic | climate

As the earth's climate has warmed, the Pacific sector of the Arctic Ocean has experienced dramatic changes, particularly the wide and shallow Chukchi Sea north of Bering Strait. The persistence of sea ice has decreased markedly due to earlier melt back and later freeze up (1), the input of warmer and fresher Pacific water through Bering Strait has increased (2), and air–sea buoyancy fluxes have led to enhanced heat gain in spring (3). These changes are significantly altering hydrographic patterns and structure over the Chukchi Shelf, as well as the timing and extent of biological production and the biogeographic boundaries of species at all trophic levels, driving an unprecedented regime shift in this ecosystem (4).

Many organisms will spread and flourish in Arctic waters as a result of climate warming, but few present as significant a threat to human and ecosystem health as *Alexandrium catenella**, a harmful algal bloom (HAB) species that produces paralytic shellfish toxins (PSTs)—one of the most potent and globally widespread of all HAB toxin families (5).

There is a long history of PST-related illness and fatality events in southeastern Alaska and along the Aleutian Islands, some dating back more than 200 y (6–9). North of the Bering Strait, however, observations of this species are scattered and few. Near Point Barrow, high concentrations (~3,000 to 16,000 cells · L^{-1}) of *A. catenella* (then called *Goniaulax tamarensis*) vegetative cells were recorded in 1954 (10), yet surveys in subsequent decades did not detect this species (11, 12). In 2003, Walsh et al. (13) reported low concentrations in the Bering Strait and on the Chukchi Shelf. More recently, Gu et al. (14) conducted morphological and phylogenetic analysis on cultures established from Chukchi Sea sediments, definitively confirming the presence and toxicity of *A. catenella* in the region. Soon after, Natsuike et al. (15) reported high concentrations of *A. catenella* resting cysts in sediments of the eastern Chukchi Sea, as well as vegetative cells of this species in surface waters (16). At that time, these cyst concentrations represented the highest levels yet recorded, indicating that a dense cyst population of unknown spatial extent existed in the Chukchi Sea.

Significance

The neurotoxin-producing dinoflagellate *Alexandrium catenella* is shown to be distributed widely and at high concentrations in bottom sediments and surface waters of the Alaskan Arctic. Future blooms are likely to be large and frequent given hydrographic and bathymetric features that support high cell and cyst accumulations, and warming temperatures that promote bloom initiation from cysts in bottom sediments and cell division in surface waters. As the region undergoes an unprecedented regime shift, the exceptionally widespread and dense cyst and cell distributions represent a significant threat to Arctic communities that are heavily dependent upon subsistence harvesting of marine resources. These observations also highlight how warming can facilitate range expansions of harmful algal bloom species into waters where temperatures were formerly unfavorable.

Author contributions: D.M.A., R.S.P., M.L.R., M.L.B., and K.L. designed research; D.M.A., E.F., R.S.P., P.L., V.U., L.M., F.B., K.L., J.M.G., Y.L., and Y.F. performed research; S.L.D. compiled and contributed hydrographic data; D.M.A., E.F., R.S.P., P.L., A.D.F., M.L.B., L.M., and F.B. analyzed data; and D.M.A., E.F., R.S.P., A.D.F., M.L.R., M.L.B., K.L., S.L.D., and J.M.G. wrote/edited the paper.

The authors declare no competing interest.

This article is a PNAS Direct Submission.

[1]To whom correspondence may be addressed. Email: danderson@whoi.edu.

This article contains supporting information online at https://www.pnas.org/lookup/suppl/doi:10.1073/pnas.2107387118/-/DCSupplemental.

Published October 4, 2021.

*Gu et al. (14) analyzed 55 strains of *Alexandrium tamarense* complex from the Chukchi Sea and concluded that they belong to *Alexandrium tamarense* Group 1 (66). Subsequently, all *Alexandrium* species within the species complex were the subject of a reclassification (67, 68) that determined that *A. catenella* has nomenclatural priority over *A. fundyense*.

Shore-based records of HABs in the Alaskan Arctic are scarce, with the exception of folklore cited by Fair and Ningeulook (17), describing Ipnauraq (north shore of the Seward Peninsula) as "the location of a red tide at one time which caused many deaths." No details are provided on symptomology or timing. More recent reports [e.g., Lefebvre et al. (18)] document PSTs in seals, walruses, sea lions, whales, and other marine mammals throughout the coast of Alaska, including in the Bering, Chukchi, and Beaufort Seas. PSTs have also been implicated but not confirmed as the cause of seabird and walrus mortalities (19, 20). The baseline picture is of blooms of *A. catenella* occurring on a sporadic basis in Alaskan Arctic waters over the last 65+ years but not to the extent where they have been recognized as a significant threat to human and ecosystem health in the region.

In this study, the distributions of both cysts and planktonic vegetative cells of *A. catenella* are presented from the Chukchi Sea and adjacent waters in 2018 and 2019. These are related to hydrographic and circulation patterns that enhance the mechanisms for bloom formation north of the Bering Strait. This extensive, multiyear field program documented a massive regional cyst bed that is unprecedented globally, as well as equally large and dense vegetative cell blooms. While we lack the long-term observations needed to definitively link these blooms to climate change, it seems likely that shifting regimes are leading to an Arctic environment increasingly hospitable to *A. catenella* bloom formation and persistence. This recently characterized *A. catenella* population represents a serious and growing threat to Alaskan Arctic communities who are justifiably concerned about their health and the health of the ecosystems on which they depend for food in a region where biotoxin-monitoring programs are often not feasible.

Results

Cyst Distribution in Sediments. *A. catenella* spends the majority of its life cycle as a resting cyst in benthic accumulations ("cyst beds") where the cysts cycle between successive states of dormancy and quiescence. They germinate (21) when conditions (e.g., temperature and oxygen) are favorable, producing motile vegetative cells that photosynthesize, divide asexually, and form the blooms that produce PSTs (5).

The regional bloom dynamics of this species are highly dependent on the distribution and abundance of resting cysts (5, 22, 23). Distributional data provide an indication of the potential size of the bloom inoculum as well as the areas where localized germination and population development may occur. Fig. 1 shows a composite distribution map of live *A. catenella* cysts based on sediment samples from cruises in 2018 (summer and fall) and 2019 (summer) in the Northern Bering Sea (NBS), Bering Strait, Chukchi Sea, and Beaufort Sea (24, 25). Since the cruises occurred at different times in two different years and covered different regions, a composite map was generated to include all samples, with cyst counts from overlapping transects averaged. This approach reveals the full spatial extent of the *A. catenella* cyst distribution and general levels of cyst abundance.

The cyst distribution stretched ~1,000 km along the coast, beginning just south of the Bering Strait and extending beyond Barrow Canyon to the western edge of the Beaufort Sea (Fig. 1). Dense cyst accumulations were seen as far as 350 km offshore and likely persist further west into unsampled Russian waters. Two distinct cyst beds are evident. The first is centered offshore of Ledyard Bay (herein called the Ledyard Bay area), extending northeast to Icy Cape and south to Kotzebue Sound and the Northern Bering Sea, with average shelf depths of 40 to 50 m. This feature is termed the Ledyard Bay cyst bed. The second (the Barrow cyst bed) lies near Barrow Canyon, with the highest abundances east of the mouth of the canyon in the western Beaufort Sea in water depths of ~50 m. Maximum concentrations were 17,600 and 14,800 cysts · cm^{-3} in the Ledyard Bay and

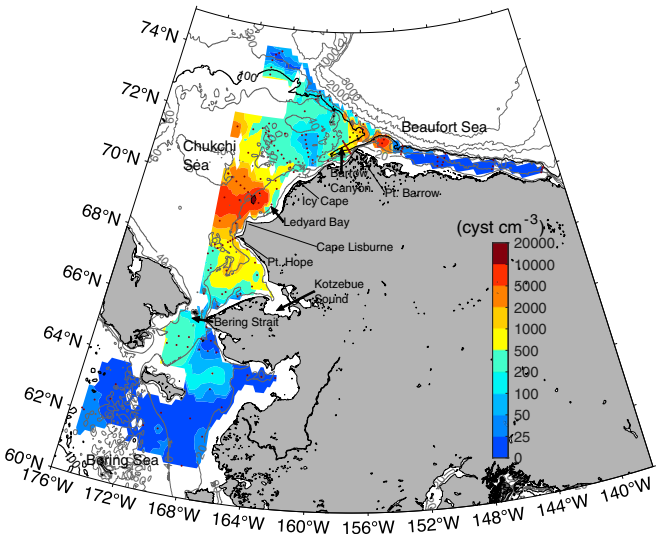

Fig. 1. Composite *A. catenella* cyst distribution and abundance in surface sediments (0 to 3 cm) for 2018 and 2019. Data points are indicated by black dots, black lines are the 100-m isobath, and gray contours are bottom depth in meters from ETOPO-2.

Barrow cyst beds, respectively. The total area of the cyst beds (defined as the area containing 300 cysts · cm^{-3} or higher) was 145,600 km^2, with the Ledyard Bay cyst bed at 128,100 km^2 and the smaller Barrow cyst bed at 17,500 km^2 (Table 1). The total number of *A. catenella* cysts within the top 3 cm of the entire Alaskan Arctic cyst bed was 7.67×10^{18}. Cysts typically germinate from a thin (few millimeters) layer at the sediment surface where there is oxygen (26), but cysts in deeper layers can contribute to bloom initiation following bioturbation or current-driven resuspension. There is active sediment mixing throughout this region (27–29), so the top 3 cm are tabulated here. Metrics for the Gulf of Maine cyst bed, a well-studied feature with a long history of seeding large-scale *A. catenella* blooms (30, 31), are presented in Table 1 for comparison.

Vegetative Cells in Surface Waters. Dense blooms of vegetative *A. catenella* cells were observed from August to early September in 2018 and 2019 (Fig. 2) (25). A November cruise in 2018 found virtually no vegetative cells anywhere in the region, highlighting bloom seasonality.

The 2018 and 2019 blooms both had dangerously high cell densities and covered large areas but were distributed differently. During both years, vegetative cells were sparsely observed south of the Bering Strait. In 2018, the main bloom was centered in the Ledyard Bay area, in close proximity to the cyst bed (Figs. 2*A* and 3), stretching along the entirety of that transect (150 km). Given that high cell counts were observed at the westernmost stations on those transects, the bloom was broader than shown, extending into unsampled Russian waters. The highest *A. catenella* cell concentrations were observed within Alaskan coastal water (ACW; Fig. 2*D*), the warmest and freshest type of Pacific summer water that passes through the Strait (*SI Appendix*). Maximum concentrations were ~5,000 cells · L^{-1} in the Ledyard Bay area, more than an order of magnitude above levels known to be dangerous (8). Cells were concentrated in the upper 20 m of the water column (Fig. 3*B*) and across large areas laterally. The exception was a near-bottom enhancement of the *A. catenella* vegetative cell population at the two inshore-most stations where cyst abundance was largest. A wind event mixed the entire water column in this region at the time, perhaps resulting in local germination due to resuspension and growth due to elevated temperatures.

Table 1. Geographic size and abundance metrics for *A. catenella* cyst beds in the Alaskan Arctic and Gulf of Maine

Region	Cyst bed area (km^2)	Total cysts × 10^{17}	Maximum cysts · cm^{-3}	Mean cysts · cm^{-3}
Ledyard Bay	128,100	65.85	17,602	1,722
Barrow	17,500	10.86	14,852	2,068
Alaskan Arctic Total	145,600	76.7	17,602	1,768
Gulf of Maine*	23,000	5.1	11,655[†]	744*

Total, maximum, and mean are for the surface 3 cm of sediment.
*Average from 2004 to 2012 (Solow et al., 2014).
[†]Maximum observed at any station from 2004 to 2012 (Anderson et al., 2014).

The 2019 *A. catenella* vegetative cell distribution was quite different. As a benefit from two nearly concurrent cruises in 2019 covering partially overlapping domains, *A. catenella* distributional data can be broken down into two intervals to show bloom progression. The first was August 4 to 19 and the second August 20 to September 11 (Fig. 2 *B*, *C*, *E*, and *F*). The highest-cell concentrations observed during early August were in a bloom patch southwest of Point Hope (Fig. 2*B*), with densities of 8,200 cells · L^{-1}. This area was also the site of significant bird mortality observed before and during the cruise, but the cause of the mortality was not determined. Highest-cell concentrations were associated with Bering summer water (BSW), a cooler, saltier

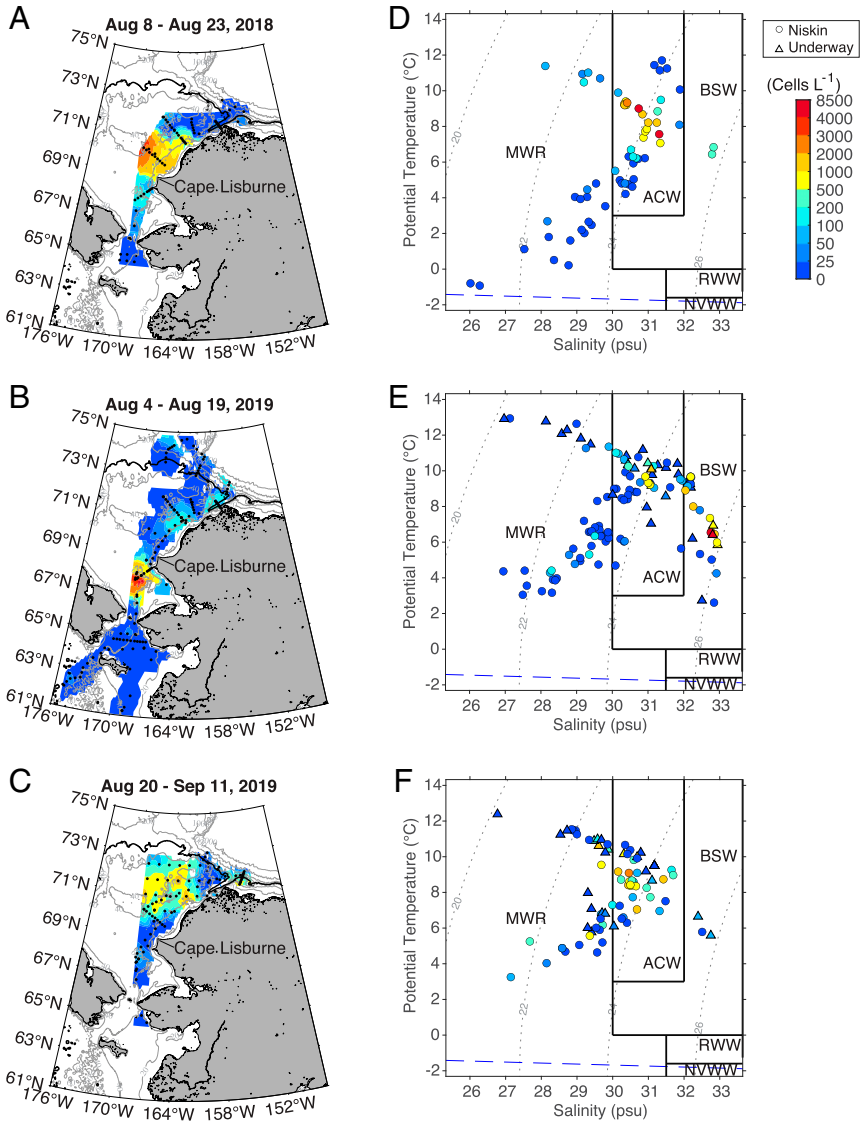

Fig. 2. Spatial distribution of vegetative *A. catenella* cells (*Left*) and associated water mass characteristics (*Right*) in surface waters for 2018 and 2019. Sampling dates are indicated above (*A*–*C*). (*A*) Summer 2018. (*B* and *C*) Summer 2019. (*D*–*F*) Temperature salinity plots showing corresponding distributions of samples within boundaries defined by major water masses (MWR = Melt Water/River runoff, RWW = Remnant Winter Water, NVWW = Newly Ventilated Winter Water, and dashed line indicates seawater freezing line). The circles indicate samples derived from surface Niskin bottles, and triangles denote underway measurements.

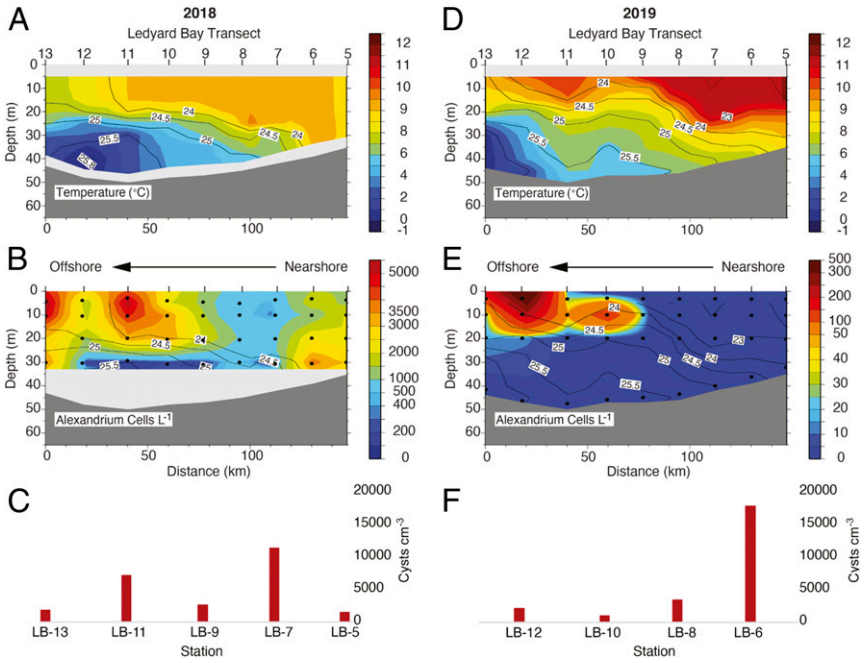

Fig. 3. Cross-sections of Ledyard Bay (LB) transects in 2018 and 2019 displaying temperature (*A* and *D*), *A. catenella* vegetative cells (cells liter^{-1}) (*B* and *E*), and cyst abundance (cysts · centimeter^{-3}) (*C* and *F*). Panels show nearshore to offshore, *Right* to *Left*, and density contours are indicated by numbers (kilograms · meter^{-3}) with white background. Note the different color scales in *B* and *E*.

type of Pacific summer water (*SI Appendix*), while moderately high cell concentrations occurred in ACW (Fig. 2*E*). Temperatures ranged from 5.6 to 9.7 °C.

Several weeks later in 2019, a large bloom was observed north of Ledyard Bay with concentrations of ∼1,000 to 2,600 cells · L^{-1} in the vicinity of Icy Cape. Highest cell densities were associated with ACW, plus a small amount of fresher, near-surface water composed of sea-ice melt, run off from the continent, and/or river water (*SI Appendix*) (Fig. 2*F*). Temperatures ranged from 5.6 to 10.0 °C. BSW was not sampled in this northern bloom, likely because this water mass had been advected to the northwest toward Herald Canyon in Russian waters (32). A third patch of cells was found east of Barrow Canyon, with concentrations of ∼1,100 cells · L^{-1}. In the Ledyard Bay area, the site of the large population in 2018, there was a smaller patch in 2019 with a maximum concentration of only ∼400 cells · L^{-1} (Fig. 2*C*). The *A. catenella* vegetative cell population was generally centered offshore and, as in 2018, most concentrated in the upper 20 m of the water column (Fig. 3*E*).

Experiments to Assess Temperature–Rate Relationships. Laboratory experiments were conducted to examine the effect of temperature on *A. catenella* cyst germination and vegetative cell growth. Sediments were collected from the Ledyard Bay area and quiescent cysts were isolated and incubated at typical in situ temperatures (0, 4, and 8.5 °C) until no further germination was observed. Germination time-course curves were fit to a log-normal cumulative distribution function using nonlinear regression, and the median germination time was derived (Fig. 4 and *SI Appendix*). Because of the difficulty of deriving a temperature–germination rate relationship from only three data points, the Chukchi Sea data were compared to well-established relationships derived for *A. catenella* cysts from the Gulf of Maine and the Nauset Marsh (Cape Cod, MA) (31) (*SI Appendix*). Strong overlap across these datasets supported their aggregation to estimate a universal temperature–germination rate relationship. The relationship can be simplified using a single metric that incorporates temperature and time: heating degree days (DD). Thus, a quiescent cyst must accumulate ∼85 DD to germinate (Fig. 4).

Vegetative growth experiments were conducted with *A. catenella* isolates from Arctic (Chukchi Sea and Greenland), subarctic (Iceland), and temperate (Gulf of Maine) regions. Growth responses were quite similar among the 12 *A. catenella* strains from these regions (*SI Appendix*, Fig. S1). Temperature had a significant influence on growth rates, with values fluctuating between 0.009 and 0.37 d^{-1}. Cells maintained at 4 °C either did not grow (though they survived) or grew very slowly. The highest growth rate (0.37 d^{-1}) was observed at 18 °C for the Chukchi isolate.

Physical Drivers. The general circulation of the Chukchi Sea is largely dictated by shelf topography. Pacific water flows northward through Bering Strait and divides into three branches, with much of the water ultimately veering eastward and draining through Barrow Canyon (Fig. 5). In summer/early fall, the eastern branch, known as the Alaskan Coastal Current (ACC), together with the Central Channel branch, account for most of the transport (33, 34). The shelf circulation is highly sensitive to wind (35). Prevailing winds are out of the northeast, which, if strong enough, are able to reverse the flow of the ACC as well as the Central Channel branch (36–38).

Pisareva et al. (39) presented a map of depth-averaged flow speed over the Chukchi Shelf using shipboard velocity data and a numerical model, demonstrating that the ACC slows considerably as it flows into the Ledyard Bay area, presumably due to the change in bottom slope adjacent to the coast. To investigate this further, a climatology of shipboard acoustic Doppler current profiler (SADCP) data on the eastern Chukchi Shelf was compiled, spanning 2002 to 2018 for the warm months of the year. This composite dataset is far more extensive than the measurements in Pisareva et al. (39). The strong flow in and to the north of the Bering Strait is the combination of the ACC and the Central Channel branch (Fig. 6). This current undergoes a stationary cyclonic meander in accordance with the bend in bathymetry at the mouth of Kotzebue Sound (note the 40-m

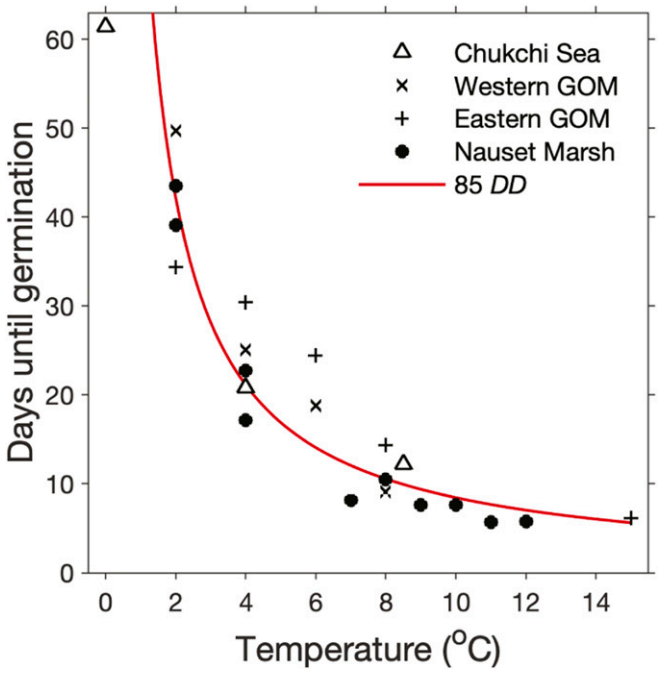

Fig. 4. Days needed for *A. catenella* cysts to germinate at laboratory incubation temperatures. Data from Chukchi Sea cyst populations are shown alongside data from cysts from western and eastern Gulf of Maine (GOM) and the Nauset Marsh on Cape Cod, MA. All experiments were conducted with quiescent (nondormant) and initially anoxic natural cyst populations exposed to oxygen during incubations. Despite their geographic separation, these cyst populations must all accumulate a mean of 85 heating degree-days (85 DD, red curve) (a metric that incorporates temperature and time) to germinate.

isobath in Fig. 6). Shortly after passing Point Hope, the flow bifurcates into the coastal and the Central Channel branches. The latter flows northward to the latitude of Hanna Shoal, where it veers eastward, flowing around both sides of the shoal before draining into Barrow Canyon.

Consistent with the flow speed map of Pisareva et al. (39), the coastal branch slows considerably north of Cape Lisburne where the isobaths diverge and speeds up again near Icy Cape where the isobaths converge (Fig. 6). The flow is weak in the Ledyard Bay area, both in the ACC and the Central Channel branch, which is conducive for the settling of material from the water column to the sediments; this is where the largest cyst bed is found. The highest counts of *A. catenella* cysts were from samples beneath the ACC where the flow is especially weak (compare Figs. 1 and 6). Cysts of several other dinoflagellate species were also most abundant in the Ledyard Bay region (*SI Appendix*, Fig. S2), indicating that the accumulation zone is a common deposition feature for dinoflagellate cysts in the region. Similarly, the circulation slows considerably as water emerges from Barrow Canyon, flowing to the east into the Barrow cyst bed (Fig. 6), which is also conducive for cyst settling.

Temperature Patterns, Germination, and Bloom Potential. To investigate bottom temperature conditions over a broad time scale, we use a recently constructed climatology of hydrographic observations in the northern Bering and Chukchi Seas (3) (*Materials and Methods*). The database spans 1922 to 2019, mainly July through mid-October. Bottom temperatures are the mean over the bottom 10 m of the water column.

The data's spatial coverage is shown in Fig. 7*A*; here, the focus is on the coastal current that advects the warmest water (red dots in the figure). The temporal and spatial variation of bottom temperatures are displayed as a time–latitude Hovmöller diagram (Fig. 7*B*). While there are gaps in the diagram due to data sparsity, it nonetheless reveals a clear signal of northward propagation of temperature in the ACC. Notably, there is a change in propagation speed near the latitude of Cape Lisburne, consistent with the current vector map (Fig. 6), which shows the flow weakening at this location. The slope of the arrows in Fig. 7*B* gives advective velocities of 13.6 and 7.7 cm $\cdot$ s^{-1} south and north of Cape Lisburne, respectively. Using the near-bottom SADCP data (Fig. 6), the average ACC velocity south of Cape Lisburne is 13.1 cm $\cdot$ s^{-1}, while to the north (excluding Barrow Canyon to be consistent with the Hovmöller calculation), the value is 8.1 cm $\cdot$ s^{-1}. This remarkable agreement in flow speeds between independent datasets strengthens our conclusion that the weakening of the flow in the Ledyard Bay area leads to the formation of the cyst bed there.

Time to *A. catenella* cyst germination was estimated from bottom water temperature climatology along the ACC track. The bulk of germination is calculated to occur between July and mid-September (Fig. 7 *B* and *C*), so blooms occurring outside this 2.5-mo window most likely originate in the south and are advected into the region. The largest in situ fluxes occur in August at 69 to 70°N within the Ledyard Bay area, where temperatures reach 8 °C and cysts germinate within ~10 d (Fig. 3). North of 71.5°N, bottom temperatures are colder, causing germination to be slower and germling fluxes to be smaller and more gradual. In the Barrow cyst bed, mean August bottom water temperature was ~3 °C (Fig. 7*B*), extending time until germination to a minimum of ~28 d (Figs. 4 and 7*C*)—one-third the rate in Ledyard Bay at the same time of year.

Effect of Warming on Bloom Potential. Are these warm temperatures a recent phenomenon? Using the hydrographic climatology, mean bottom water temperatures from 1999 to 2008 and from 2009 to 2018 were calculated for June through October (Fig. 8 *A* and *B*). Prior to 1999, the data were too sparse to provide robust estimates. Warming extends all along the ACC from the Bering Strait to Barrow Canyon, including the Central Channel branch to the latitude of Hanna Shoal (Fig. 8*C*). Significant warming has occurred in the Ledyard Bay region, where in some places the temperature has increased by nearly 4 °C.

To examine the effect of warming on the potential for *A. catenella* blooms, 5-y means of bottom temperatures from 1999 to 2018 were calculated separately for the Ledyard Bay and Barrow cyst bed regions (outlined in green in Fig. 8*D*). For the purpose of this analysis, the Ledyard Bay area is bounded between 68.8 and 70.5°N, while the Barrow cyst bed area is bounded between the 20- and 100-m isobaths and 155.5 and 153°W. Seasonally, the warmest water arrives in the Ledyard Bay area via the ACC roughly 1 mo before reaching Barrow, so temperature data were used from July to August and from August to September for these areas, respectively.

From 1999–2003 to 2014–2018, mean bottom temperatures in the Ledyard Bay cyst bed area increased from 4.2 to 6.8 °C, while near Barrow they increased from 2.1 to 3.8 °C (Fig. 9*A*). Using the temperature–germination rate relationship (Fig. 4), warming from 1999 through 2003 to 2014 through 2020 would have enhanced germling cell production 1.6- and 1.8-fold in the Ledyard Bay and Barrow cyst bed regions, respectively (Fig. 9*B*). Bottom water warming also reduced the calculated time until germination by ~20 d (Fig. 8*D*).

Discussion

A. catenella is among the most widespread and dangerous of all HAB species, with a global distribution predominantly in temperate and subarctic waters (5). While this species has been recorded sporadically in the Alaskan Arctic (10, 13), these observations have been rare and are interspersed with many years

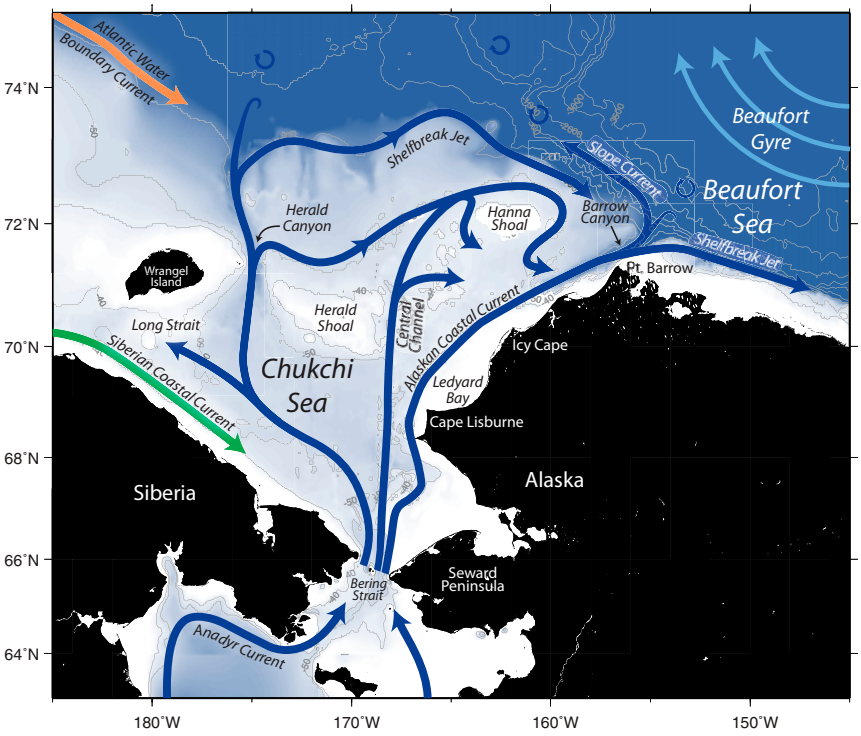

Fig. 5. Schematic circulation of the Chukchi Sea (69). The bottom topography is from ETOPO-2.

of no species reports (11, 12). More recent observations (16) of planktonic *A. catenella* cells within and north of the Bering Strait have been interpreted as evidence that Arctic blooms are episodically advected northward through the Strait in Pacific summer water. Here, we document massive accumulations of resting cysts of this species across large areas of the Alaskan Arctic over two successive years, as well as widespread and dense surface water blooms of the vegetative cells that are the dominant source of toxins in the marine food web. Two mechanisms for toxic blooms in the Chukchi Sea are suggested, one reliant on in situ bloom initiation and development in the Ledyard Bay and Barrow regions, and the second on populations transported through Bering Strait from southern waters. The retentive effect of hydrography and bathymetry in the Ledyard Bay and Barrow areas, combined with warming temperatures that support both in situ cyst germination and vegetative cell growth, suggest that annually recurrent, self-initiating bloom events are already occurring and are increasingly probable.

Cyst Distribution and Abundance. The *A. catenella* cyst distribution in the Alaskan Arctic (Fig. 1) is the densest and geographically largest known feature of its type globally. Because of international restrictions preventing US vessels from sampling Russian waters, this feature is likely more expansive than shown here. The general configuration is that of two distinct cyst beds separated by areas with low abundances (Fig. 1). East of Point Barrow in the Beaufort Sea, cysts are less abundant but still present along the Beaufort Shelf. A slowing of currents in the Ledyard Bay region (Fig. 6) is conducive to cyst deposition, consistent with the size and persistence of this feature through time. Current velocities also decrease substantially in the area of the Barrow cyst bed, which is located near a known bowhead whale hotspot—a recurrent feature associated with fronts and dense aggregations of zooplankton (40). Hydrographic fronts are known to be sites for aggregations of motile dinoflagellates and for deposition of their cysts (41).

Cyst density and distribution can be important metrics for predicting *A. catenella* bloom occurrence (42, 43), and the massive scale of the cyst bed described here raises major concerns about future bloom potential in the Alaskan Arctic. Abundances reported here are similar to, but larger than, observations from Ledyard Bay in 2010 [10,600 cysts · cm^{-3} maximum (15)] and, with one exception, are denser than the highest concentrations reported for *A. catenella* cysts globally. The only higher count is from the nearby Russian coast of the NBS, where Orlova and Morozova (9) report concentrations of 25,860 cysts · cm^{-3} at one location. In the Gulf of Maine, a region with what was until now the world's largest documented *A. catenella* cyst bed in area and overall abundance, the mean cyst bed size from 2004 to 2012 was 23,000 km^2 with 5.1×10^{17} total cysts. The estimated cyst abundance in the Alaskan Arctic is thus 15 times greater, and the total spatial extent of the cyst bed 6.3 times larger (Table 1). As small as it might seem in retrospect, the Gulf of Maine cyst bed has sustained large-scale, annually recurrent blooms and dangerous levels of shellfish toxicity for decades (42, 44–46). The same seems likely in the Alaskan Arctic going forward.

Vegetative Cell Distribution, Abundance, and Origin. Alaskan Arctic blooms of motile, vegetative *A. catenella* cells were also notable in scale and density. The 2018 bloom (Fig. 2) stretched at least 200 km adjacent to the coast and extended more than 150-km offshore and likely further outside the survey area. In the most intense patches, cells were distributed throughout at least the upper 20 m of the water column, representing a large reservoir of toxin to both planktonic and benthic food webs. For comparison, a large *A. catenella* bloom in 2005 that closed shellfish beds from central Maine to Massachusetts was about half as large in alongshore and offshore dimensions or 25% in total area (47). Furthermore, maximum cell concentrations in the 2019 Arctic

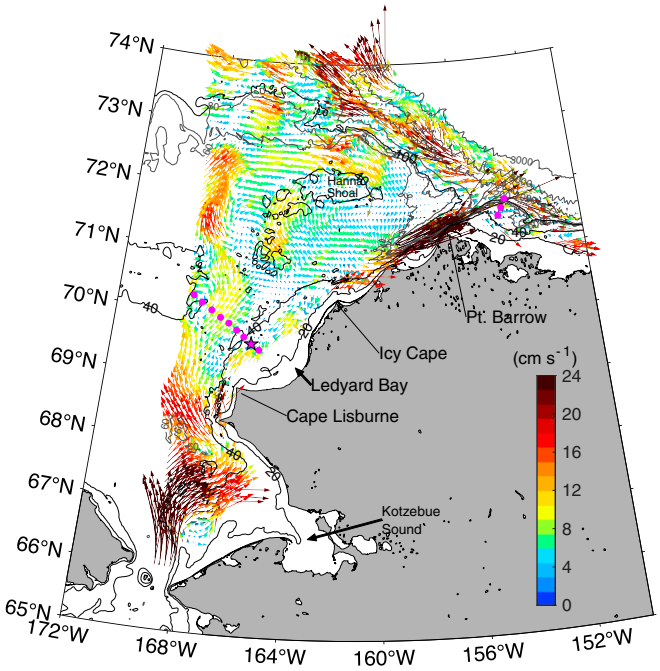

Fig. 6. Time-mean, depth-averaged flow vectors using the composite SADCP dataset. Vector length and color indicate speed. The Ledyard Bay station positions are indicated by the magenta circles, as are the Barrow station positions on the western Beaufort Shelf. Bottom topography is from IBCAO v3 (International Bathymetric Chart of the Arctic Ocean, version 3).

bloom were four times higher than in the open Gulf of Maine in 2005. Higher *A. catenella* cell concentrations are observed elsewhere in fjords, bays, or localized areas globally [e.g., Brosnahan et al. (48)], but these Alaskan values are notably high for open coastal waters.

Two mechanisms, acting either separately or concurrently, are proposed for the origin of these blooms. One is suggested by the observations of Natsuike et al. (49) and by our 2019 vegetative cell distributions (Fig. 2*B*). In both cases, patches of cells were observed within the strong poleward flow emanating from Bering Strait (Fig. 6), suggesting advection into the Strait and the Chukchi Sea from established blooms in southern waters. Natsuike et al. (49) argued that the blooms were carried within Pacific summer water (they did not distinguish specific water masses). Our 2019 data reveal that the highest cell concentrations west of Point Hope were within BSW (Fig. 2*E*). This water mass has higher nutrients than ACW and hence is more apt to spur bloom activity. Orlova and Morozova (9) report high *A. catenella* cyst abundances at several locations along the Russian shore of the Bering Sea, so northward advection of blooms associated with these populations may occur through Bering Strait via the Anadyr Current. The water in the current is one of the constituents of BSW that flows offshore of the ACC, which explains why we sampled it at the seaward end of the Point Hope transect in Fig. 2*B*.

One approach to investigations of the dispersal and connectivity of *A. catenella* populations is via the saxitoxin congener profile of isolates from different regions, as these are considered constitutive markers for populations. Saxitoxin composition data are available for isolates along the western coast of the Bering Sea (50) and for the eastern Bering Sea and the Chukchi Sea (14, 49). Available profiles and a discussion of implications are given in the *SI Appendix*. One preliminary conclusion from this limited dataset is that the Ledyard Bay cyst bed may derive, at least in part, from cells transported from the western Bering Sea via the Anadyr Current and not from the eastern Bering Sea. Given order-of-magnitude differences in toxicity among saxitoxin congeners, the human health and ecosystem implications are profound and provide strong justification for further study of population connectivity.

The overlap between regions of high cyst abundance with warm bottom water temperatures strongly supports a second mechanism: that blooms originate locally in the Ledyard Bay area and just east of Barrow Canyon through localized cyst germination. Vegetative cells were observed in close proximity to the Ledyard Bay cyst bed at a time when bottom and surface

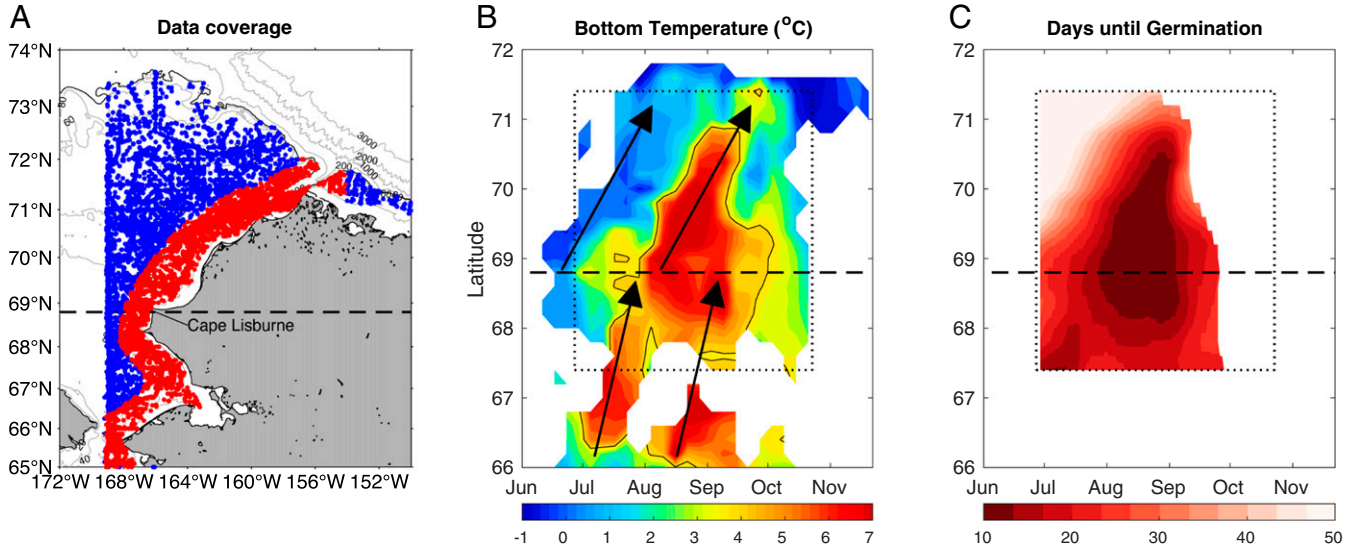

Fig. 7. Hovmöller analysis of regional hydrography. (*A*) Spatial coverage of the hydrographic climatological data. Red dots denote the coastal region used in the construction of the Hovmöller plot. The dashed line corresponds to the latitude of Cape Lisburne. (*B*) Latitude versus mo Hovmöller plot of bottom water temperature (color, Celsius) for the ACC (red dots in *A*). The 4 °C isotherm is contoured. The arrows denote the propagation of temperature signals. (*C*) Days at the in situ bottom water temperature until *A. catenella* cysts germinate, within the dashed box of (*B*). This is calculated from interpolated in situ temperatures and the germination requirement of 85 DD (Fig. 4). If days until germination exceed 100 d, these cysts will not germinate in time to seed a bloom during the summer growing season, so white is shown.

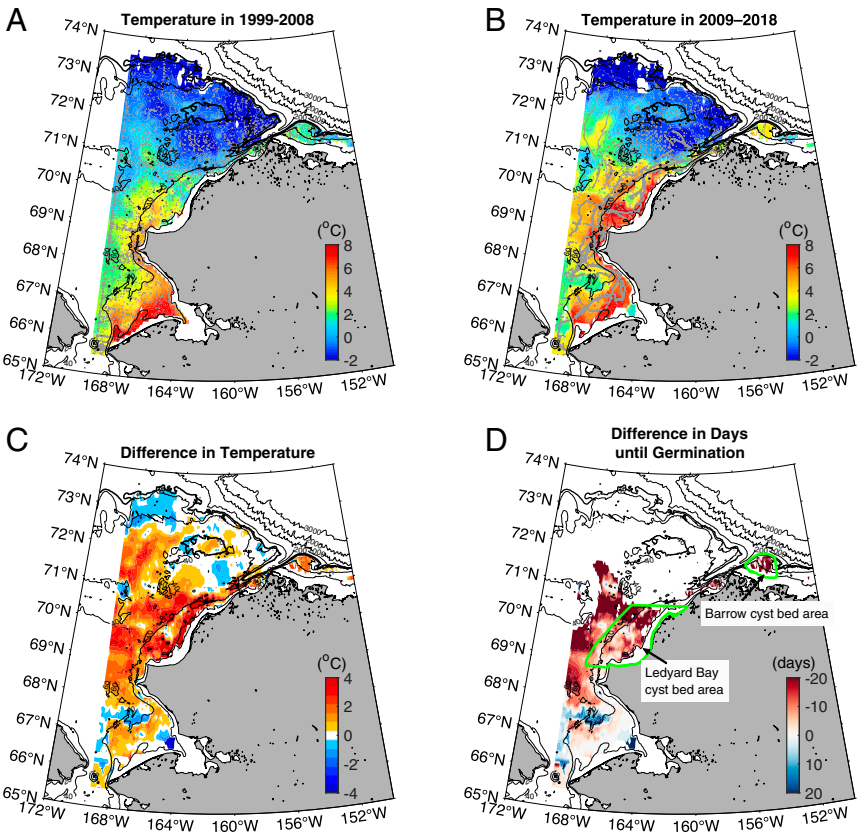

Fig. 8. Mean bottom water temperature for 1999 to 2008 (*A*) and 2009 to 2018 (*B*), calculated from the hydrographic climatological data (gray dots) for June to October. The difference between the later and earlier periods is shown for temperature (*C*) and the difference in the mean number of days needed at the mean temperature (*D*) for *A. catenella* cysts to germinate. Germination calculations are based on the 85-DD threshold required for cysts to germinate (Fig. 4). If the days until germination exceed 100 d, white is shown. Ledyard Bay and Barrow cyst bed areas are bounded in green.

water temperatures were at levels that support rapid cyst germination and cell division. A direct link between the Barrow cyst bed and the bloom observed there in 2019 (Fig. 2*C*) is less clear because of generally colder bottom temperatures (Fig. 9*A*) but still possible.

In either case, whether blooms arise from local cyst germination or are delivered from bloom populations to the south, or most likely, some combination of the two, our survey data document surface temperatures ranging from 6 to 12 °C in both 2018 and 2019, a range at which laboratory cultures of Chukchi isolates of *A. catenella* grow at 50 to 75% of their maximal rates (51, 52) (*SI Appendix*, Fig. S1).

The 2019 *A. catenella* vegetative cell distribution suggests that both bloom formation mechanisms are at work. The first observations of a bloom southwest of Pt. Hope just north of the Bering Strait in early August (Fig. 2*B*) indicates an advected population, whereas the (less intense) bloom observed almost a month later in the vicinity of Icy Cape (Fig. 2*C*) more likely originated from local cyst germination, perhaps augmented with advected cells. As previously noted, the Point Hope population was in BSW (Fig. 2*E*), which likely was subsequently transported northwest toward Herald Canyon (32, 53). By contrast, the bloom that occurred several weeks later near Icy Cape was associated with warmer and fresher ACW (Fig. 2*F*), which flows closer to the coast. The mean circulation map (Fig. 6) indicates that it should take much longer for a parcel to advect from Point Hope to Icy Cape (~50 d) than the time between occupation of the two transects (~25 d). The same conclusion is reached using synoptic SADCP data collected during the first 2019 cruise (53). Notably, a signature of the Icy Cape bloom was developing during the early cruise (Fig. 2*B*), adding further credence that it developed via local cyst germination.

Cyst Bed Formation. What then is the fate of cysts formed by these blooms, and why are the cyst beds so dense? One explanation is suggested by the "trail of death" hypothesis described for zooplankton transported from southern waters into the Arctic, where cold temperatures prevent life cycle completion (54). Applied to *A. catenella*, we can hypothesize that blooms advected by relatively warm surface waters would form cysts that deposit in bottom sediments, where temperatures are too cold to support significant germination the following year. Viable cysts would theoretically accumulate through time to very high levels because of the imbalance between inputs and losses, creating a substantial and growing seedbed. *A. catenella* cysts in bottom sediments can survive from decades (55) to a century (56), so this type of "sleeping giant" Arctic cyst bed would represent a significant and dangerous site for in situ bloom inoculation as waters warm.

Though likely an apt description of conditions in the near past, this hypothesis does not fit our recent observations. Bottom temperatures even two decades ago were likely too cold to support significant cyst germination, but emerging temperature patterns, both those observed concurrently with blooms in situ (Figs. 3 and 4) (53, 57, 58) and those calculated using historical data (Figs. 7 and 8), can drive rapid cyst germination and substantial germling fluxes. Mean bottom water temperatures have warmed significantly over the last two decades (Fig. 9*A*), increasing ~2.5 and 1.7 °C in the Ledyard Bay and Barrow regions, respectively (Fig. 9*A*). When this temperature increase is applied to the temperature–germination rate relationship for *A. catenella* cysts (Fig. 4), a nearly twofold

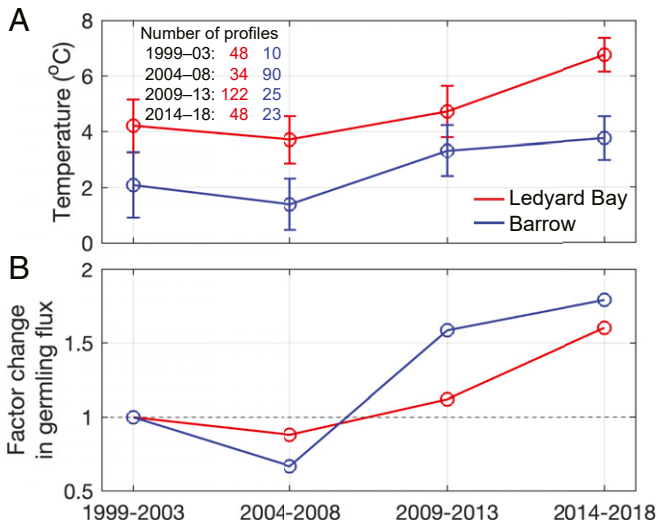

Fig. 9. Effect of bottom water temperature change on *A. catenella* germling cell production in Alaskan Arctic cyst bed areas. (*A*) Mean temperature in July to August and August to September in the Ledyard Bay and Barrow cyst bed areas, respectively. Number of profiles in each period is indicated in the upper left. Data were binned in 5-y intervals to ensure a relatively even data coverage of the summer months. (*B*) Factor change in the germling cell flux from 1999 to 2003 values.

increase in germling production is estimated in both cyst bed areas (Fig. 9*B*). To place that increase in context, in the Gulf of Maine, where a direct relationship between cyst abundance and the geographic extent of *A. catenella* toxicity has been established (42, 43), a twofold increase in germling production would result in a 2.3-fold increase in the length of coastline closed to shellfish harvesting because of PSTs and a 6.5-fold increase in the cumulative shellfish toxicity (42).

Warming temperatures have also advanced and expanded the temporal window during which blooms can form. With the decadal warming documented in Fig. 9*A*, ∼20 fewer days would be needed for a cyst to germinate in the Ledyard Bay and Barrow regions than in the prior decade (Fig. 8*D*). With doubling times of 2.5 to 4.5 d at the temperatures observed in Ledyard Bay in August 2018 to 2019 (Fig. 3 *A* and *D* and *SI Appendix*, Fig. S2*A*), significant additional population development would be possible during the 20-d "head start." Thus, the recent warming supports earlier and faster germination, longer periods favorable to planktonic blooms, and more rapid cell division and bloom development, thereby dramatically increasing the potential for local initiation of blooms from Alaskan Arctic cyst beds. Continued warming will further enhance bloom potential in the region through these complementary mechanisms.

Given observations of extremely high cyst concentrations in 2010 (15) as well as our own more recent observations of similar and higher-cyst abundances (Fig. 1), it appears that the Alaskan Arctic cyst beds are persistent features, as has been observed for this species in the Gulf of Maine (42, 59).

The persistence of extremely high cyst concentrations in Chukchi bottom sediments for a decade or longer under conditions that support substantial cyst germination might reflect several factors. One is simply replenishment of the cyst population through completion of the full life cycle in the region of the cyst bed [i.e., cysts germinate, and vegetative cells grow in the same general area without significant advective losses, consistent with the retentive current flows observed for the region and the high vegetative cell densities (Fig. 6)]. Alternatively, if advected blooms augment the size of the self-initiating blooms, cyst deposition could be much larger than would be the case with in situ bloom development alone.

Summary and Conclusions. Recent surveys have revealed massive deposits of *A. catenella* resting cysts in bottom sediments of the Alaskan Arctic, as well as abundant vegetative cells in the water column during summer months. Two mechanisms are proposed to explain the origins of the blooms, one reliant on the previously hypothesized advection of established *A. catenella* populations from waters south of the Bering Strait, and the second, more worrisome, being a new concept of intensifying in situ germination from the cyst bed, which is likely to have been long dormant until the region's recent warming. Warming of surface waters similarly enhances vegetative cell growth and bloom development. It is likely that both advection and germination-driven mechanisms operate concurrently at times.

These data suggest that there will be recurrent, locally originating, and self-seeding blooms of *A. catenella* in the Alaskan Arctic going forward. This argument is based in part on striking similarities between patterns of cysts, vegetative cells, and hydrography in the Alaskan Arctic and the Gulf of Maine, the latter a well-studied region with a history of large-scale, annually recurrent toxic blooms lasting many decades (47, 48).

The implications of these findings are significant in several ways. First, they document a significant threat to food security in the region due to the potential transfer of toxins through the food web. Second, as climate warming continues and sea ice extent decreases further, the emergence of toxic blooms represents an additional stressor to ecosystems already undergoing unprecedented changes (4, 60). Productivity on the Chukchi Shelf supports multiple trophic levels, including important subsistence harvest species such as seabirds, walruses, ice seals, and whales. *Alexandrium catenella* blooms thus represent a significant threat to Alaskan Arctic ecosystems and to the human communities that depend on these resources for food and survival.

Materials and Methods

Cruise Details. Sampling took place during Distributed Biological Observatory-Northern Chukchi Integrated Survey cruises in August 2018 and 2019 (HLY1801 and HLY1901), as well as during additional cruises of opportunity, including an Arctic Observing Network cruise (HLY1803, October to November 2018), an Arctic Integrated Ecosystem Research Program cruise (IERP, August to October 2019), and the NBS cruise (Aug to Sept 2019). Isolates used in temperature gradient bar experiments were established from cysts in sediments collected from the Chukchi Sea in 2010 (14). *SI Appendix*, Table S1 provides a complete listing of sampling efforts.

Plankton Sampling and *Alexandrium* Hybridization.

Collection and preservation. At each station, 2 L water were collected from Niskin bottle samples taken at the surface, 10 m, and chlorophyll maximum. Additional depths were sampled when significant concentrations of *Alexandrium* cells were detected through shipboard microscopy or underway imagery. During HLY1901 and IERP, the underway seawater system was used to collect additional samples during transit. Water samples were processed and preserved using formalin-methanol fixation for fluorescence in situ hybridization (FISH) analysis, as described in ref. 61 and detailed in *SI Appendix*.

Hybridization. FISH was used to label and enumerate *A. catenella* cells in the methanol-preserved samples. This approach ensures quick and accurate identification of *A. catenella* in samples that contain morphologically similar dinoflagellates that can confound identification under traditional light microscopy. Methods for sample processing and analysis followed ref. 61 and are detailed in *SI Appendix*.

Sediment Collection and Cyst Enumeration.

Collection. Sediments used for *A. catenella* cyst abundance were collected via a 0.1-m^2 weighted Van Veen grab. A syringe tube was used to capture a single 16-cm^{-3} plug of sediment, representing the 0- to 3-cm layer, from the surface of the grab. For samples collected during the IERP cruise, several plugs from the 0- to 3-cm layer were homogenized prior to analysis. Sediment was homogenized and stored in an airtight container maintained in the dark at 1 to 4 °C. Methods for sample processing and cyst enumeration

followed Anderson et al. (42) and are detailed in *SI Appendix*. All counts were normalized to cysts per cubic centimeter (cysts · cm^{-3}).

Regional Cyst Bed Abundance Estimates. To estimate overall cyst abundance within the study region, data from all cruises were combined, with repeat stations averaged, to create a composite cyst dataset. The area corresponding to cyst concentrations > 300 cysts · cm^{-3} was estimated using a gridded lateral map of cyst abundance as described under *Construction of Lateral Maps and Vertical Sections*. This was used to estimate the total cyst load within the top 3 cm of each cyst bed region as well as across the entire study area.

Hydrographic Analyses. Conductivity–temperature–depth (CTD) data were collected during HLY1801, HLY1901, and HLY1803, using *Healy*'s Sea-Bird 911plus CTD. The CTD was mounted on a 24-position rosette with 10-L Niskin bottles. Bottle salinity samples were taken for conductivity sensor assessment and calibration when appropriate. Laboratory calibrations for CTD sensors were performed by the manufacturer prior to and after each field season. Resulting data quality from all cruises was excellent, and downcast 1-db pressure-averaged files had resulting accuracies near 0.001 °C for temperature and 0.002 for salinity.

SADCP Database. The SADCP dataset includes 33 cruises from Unitied States Coast Guard Cutter (USCGC) *Healy* and 7 cruises each from R/V *Sikuliaq* and R/V *Mirai* between 2002 and 2018. All *Sikuliaq* cruises, and *Healy* cruises after 2004, were collected with the University of Hawaii Data Acquisition System (UHDAS) software. The *Mirai* and the 2002 to 2004 *Healy* SADCP data were collected with Vessel-Mounted Data Acquisition Software (VMDAS). Both sets were further edited based on consideration of standard status variables, including "percent good" and "error velocity." Only on-station data were used for the 2017 cruise due to calibration problems. A significant portion of the 2002 to 2004 *Healy* underway data was edited out as well. A concern for all ships was the so-called "forward bias:" Under poor conditions, the measured ADCP velocity relative to the transducer can drift toward zero, producing a bias in the direction of the ship's motion. We adopted a conservative approach to transmit data, requiring additional evidence that they were valid rather than only looking for obvious errors.

Historical Hydrographic Database. Water column hydrographic profile data were obtained from the compilation described in ref. 3. All data were processed from raw form by the originating institutions and subject to additional screening procedures outlined therein.

Construction of Lateral Maps and Vertical Sections. To make the lateral maps, the data were interpolated onto a regular grid following the procedure used in Davis (62) and Våge et al. (63). Enhanced weighting was given to data in the along-isobath direction. This is appropriate given the predominantly barotropic circulation in the study region. For the lateral temperature and velocity maps, an effective radius of 30 km was used, and the grid spacing was 0.1° × 0.1°. Since the biological (cyst and cell) data coverage is considerably more sparse, an effective radius of 120 km was used, with a lateral grid resolution of 0.2° × 0.2°. For the vertical sections, Laplacian spline interpolation (64) was used with 10-km horizontal and 5-m vertical grid spacing.

Temperature Gradient Bar Experiments. Laboratory experiments assessed the effects of temperature on *A. catenella* germination and growth under temperature conditions that bloom populations would experience during summer in the Alaskan Arctic. Germination experiments were conducted with cyst-rich sediment collected from Ledyard Bay at LB-6 (69.584°N and −165.7427°E) and LB-8 (69.785°N and −166.452°E) on August 22, 2019. Sediment was stored at 0 °C under anoxic conditions until June 2020, then diluted with naturally oxygenated f/2 media to create a large, homogenized slurry for aliquoting. Slurry subsamples were delivered to 34 glass flasks as detailed in ref. 31. Four flasks were immediately harvested to determine initial cyst concentration. The remaining flasks were randomly placed in incubators set to 0, 4, and 9 °C. Illumination was set to 24 h at low light levels (~0.75 μmol · m^{-2} · sec^{-1}) to match light conditions experienced in Ledyard Bay during summer. Sampling intervals varied between incubation temperatures to ensure adequate coverage of the germination time course and ranged from 3 to 15 d. At each harvest interval, the flasks to be harvested were thoroughly rinsed and their contents prepared for counting by staining with primulin as in ref. 65. All uncounted slurries were thoroughly mixed biweekly to provide consistent exposure to light and oxygenated media. To calculate the percentage of cysts that germinated over each time interval, the remaining cysts at each harvest interval were subtracted from the average initial cyst concentration.

Data Availability. Physical and environmental data collected during research cruises in 2018 to 2019 have been deposited in the Arctic Data Center repository (10.18739/A2D21RK4M, 10.18739/A28C9R51P, and 10.18739/A2HT2GC7Z) (24, 25, 53). Data on *Alexandrium catenella* cyst and cell abundance is available at the Arctic Data Center repository (10.18739/A2W66993S, 10.18739/A2RF5KG8) (57, 58). All other study data are included in the article and/or supporting information.

ACKNOWLEDGMENTS. We acknowledge that the western and northern coasts of Alaska, along which this research was conducted, are the ancestral lands of the Yup'ik and Iñupiat People past, present, and future. We honor with gratitude these lands and waters and the Yup'ik and Iñupiat People. We gratefully acknowledge the following: Lee Cooper, Christina Goethel, Caitlin Meadows, and Laura Gemery for benthic sampling assistance; Matthew Capucci, Madison Shankle, and Anna Apostel for plankton sampling; Olga Kosnyrev and Valery Kosnyrev for cyst mapping support; Finn Morrison for cruise preparation and sample processing; Anna Mounsey for IERP sample collection; and the USCGC *Healy* crew and Ship-based Science Technical Support in the Arctic (STARC) technicians for general shipboard assistance. Thanks also to Hai-Feng Gu for generously providing sediments collected from the Chukchi Sea. Funding for D.M.A., R.S.P., E.F., P.L., A.D.F., V.U., M.L.B., L.M., F.B., and M.L.R. was provided by grants from the NSF Office of Polar Programs (Grants OPP-1823002 and OPP-1733564) and the National Ocanic and Atmospheric Administration (NOAA) Arctic Research program (through the Cooperative Institute for the North Atlantic Region [CINAR; Grants NA14OAR4320158 and NA19OAR4320074]), for J.M.G. through CINAR 22309.07 UMCES (University of Maryland Center for Environmental Science), and for D.M.A. and K.L. through NOAA's Center for Coastal and Ocean Studies Ecology and Oceanography of Harmful Algal Blooms (ECOHAB) Program (NA20NOS4780195). Funding for D.M.A., M.L.R., M.L.B., E.F., V.U., and A.D.F. was also provided by NSF (Grant OCE-1840381) and NIH (Grant 1P01-ES028938-01) through the Woods Hole Center for Oceans and Human Health. S.L.D. was supported by North Pacific Research Board IERP Grants A91-99a and A91-00a. This is IERP publication ArcticIERP-41 and ECOHAB Contribution No. ECO983.

1. K. E. Frey, J. A. Maslanik, J. Clement Kinney, W. Maslowski, "Recent variability in sea ice cover, age, and thickness in the Pacific Arctic Region" in *The Pacific Arctic Region: Ecosystem Status and Trends in a Rapidly Changing Environment*, J. M. Grebmeier, W. Maslowski, Eds. (Springer Netherlands, Dordrecht, 2014), pp. 31–63.
2. R. A. Woodgate, Increases in the Pacific inflow to the Arctic from 1990 to 2015, and insights into seasonal trends and driving mechanisms from year-round Bering Strait mooring data. *Prog. Oceanogr.* **160**, 124–154 (2018).
3. S. L. Danielson *et al*., Manifestation and consequences of warming and altered heat fluxes over the Bering and Chukchi Sea continental shelves. *Deep Sea Res. Part II Top. Stud. Oceanogr.* **177**, 104781, 10.1016/j.dsr2.2020.104781 (2020).
4. H. P. Huntington *et al*., Evidence suggests potential transformation of the Pacific Arctic ecosystem is underway. *Nat. Clim. Chang.* **10**, 342–348 (2020).
5. D. M. Anderson *et al*., The globally distributed genus *Alexandrium*: Multifaceted roles in marine ecosystems and impacts on human health. *Harmful Algae* **14**, 10–35 (2012).
6. A. J. Lewitus *et al*., *Harmful Algal Blooms Along the North American West Coast Region: History, Trends, Causes, and Impacts* (Elsevier, 2012).
7. R. L. RaLonde, *Harmful Algal Blooms on the North American West Coast: Proceedings of Harmful Algal Blooms (HABs), The Encroaching Menace, A Conference to Organize a West Coast Effort for Monitoring and Research on Harmful Algal Blooms, Held January 1999, Anchorage, Alaska, Report; no. AK-SG-01-05* (University of Alaska Sea Grant College Program, Fairbanks, Alaska, 2001).
8. M. W. Vandersea *et al*., Environmental factors influencing the distribution and abundance of *Alexandrium catenella* in Kachemak Bay and lower Cook Inlet, Alaska. *Harmful Algae* **77**, 81–92 (2018).
9. T. Y. Orlova, T. V. Morozova, Dinoflagellate cysts of the genus *Alexandrium halim*, 1960 (Dinophyceae: Gonyaulacales) in recent sediments from the Northwestern Pacific Ocean. *Russ. J. Mar. Biol.* **45**, 397–407 (2019).
10. A. Bursa, Phytoplankton in coastal waters of the Arctic Ocean at Point Barrow, Alaska. *Arctic* **16**, 239–262 (1963).
11. R. Horner, G. C. Schrader, Relative contributions of ice algae, phytoplankton, and benthic microalgae to primary production in nearshore regions of the Beaufort Sea. *Arctic* **35**, 485–503 (1982).
12. Y. B. Okolodkov, J. D. Dodge, Biodiversity and biogeography of planktonic dinoflagellates in the Arctic Ocean. *J. Exp. Mar. Biol. Ecol.* **202**, 19–27 (1996).
13. J. J. Walsh *et al*., Trophic cascades and future harmful algal blooms within ice-free Arctic Seas north of Bering Strait: A simulation analysis. *Prog. Oceanogr.* **91**, 312–343 (2011).
14. H. Gu *et al*., Morphology, phylogeny, and toxicity of Atama complex (Dinophyceae) from the Chukchi Sea. *Polar Biol.* **36**, 427–436 (2013).
15. M. Natsuike *et al*., Abundance and distribution of toxic *Alexandrium tamarense* resting cysts in the sediments of the Chukchi Sea and the eastern Bering Sea. *Harmful Algae* **27**, 52–59 (2013).

16. M. Natsuike *et al*., Possible spreading of toxic *Alexandrium tamarense* blooms on the Chukchi Sea shelf with the inflow of Pacific summer water due to climatic warming. *Harmful Algae* **61**, 80–86 (2017).
17. Bering Land Bridge National Preserve, Alaska. https://nps.maps.arcgis.com/apps/MapJournal/index.html?appid=e1697b7555bf485fbfa15c1d36d95ddd. Accessed 24 August 2021.
18. K. A. Lefebvre *et al*., Prevalence of algal toxins in Alaskan marine mammals foraging in a changing arctic and subarctic environment. *Harmful Algae* **55**, 13–24 (2016).
19. Anonymous, *Bering Strait: Walruses and Saxitoxin—Late Summer/Fall 2017* (Alaska Sea Grant, 2017).
20. V. Shearn-Bochsler *et al*., Fatal paralytic shellfish poisoning in Kittlitz's Murrelet (Brachyramphus brevirostris) nestlings, Alaska, USA. *J. Wildl. Dis.* **50**, 933–937 (2014).
21. A. D. Fischer, M. L. Brosnahan, D. M. Anderson, Quantitative response of *Alexandrium catenella* cyst dormancy to cold exposure. *Protist* **169**, 645–661 (2018).
22. M. L. Brosnahan, A. D. Fischer, C. B. Lopez, S. K. Moore, D. M. Anderson, Cyst-forming dinoflagellates in a warming climate. *Harmful Algae* **91**, 101728 (2020).
23. S. K. Moore *et al*., Factors regulating excystment of *Alexandrium* in Puget Sound, WA, USA. *Harmful Algae* **43**, 103–110 (2015).
24. E. Fachon, D. Anderson, Alexandrium catenella planktonic cell distribution in the Alaskan Arctic (2018-2019). Arctic Data Center. https://doi.org/10.18739/A2W66993S. Deposited 10 October 2021.
25. E. Fachon, D. Anderson, Alexandrium catenella resting cyst distribution in the Alaskan Arctic (2018-2019). Arctic Data Center. https://doi.org/10.18739/A2RF5KG8J. Deposited 10 October 2021.
26. A. Ishikawa *et al*., *In situ* dynamics of cyst and vegetative cell populations of the toxic dinoflagellate *Alexandrium catenella* in Ago Bay, central Japan. *J. Plankton Res.* **36**, 1333–1343 (2014).
27. M. Baskaran, A. S. Naidu, 210Pb-derived chronology and the fluxes of 210Pb and 137Cs isotopes into continental shelf sediments, East Chukchi Sea, Alaskan Arctic. *Geochim. Cosmochim. Acta* **59**, 4435–4448 (1995).
28. L. W. Cooper, J. M. Grebmeier, Deposition patterns on the Chukchi shelf using radionuclide inventories in relation to surface sediment characteristics. *Deep Sea Res. Part II Top. Stud. Oceanogr.* **152**, 48–66 (2018).
29. Z. Z. A. Kuzyk, C. Gobeil, R. W. Macdonald, 210Pb and 137Cs in margin sediments of the Arctic Ocean: Controls on boundary scavenging. *Global Biogeochem. Cycles* **27**, 422–439 (2013).
30. D. M. Anderson *et al*., Harmful algae in the Gulf of Maine: Oceanography, population dynamics, and toxin transfer in the food web. *Deep Sea Res. Part II Top. Stud. Oceanogr.* **103**, 1–5 (2014).
31. D. M. Anderson, D. Townsend, D. McGillicuddy, J. Turner, The ecology and oceanography of toxic *Alexandrium fundyense* blooms in the Gulf of Maine. *Deep Sea Res. Part II Top. Stud. Oceanogr.* **52**, 2365–2876 (2005).
32. J. Linders, R. S. Pickart, G. Björk, G. W. K. Moore, On the nature and origin of water masses in Herald Canyon, Chukchi Sea: Synoptic surveys in summer 2004, 2008, and 2009. *Prog. Oceanogr.* **159**, 99–114 (2017).
33. D. Gong, R. S. Pickart, Summertime circulation in the eastern Chukchi Sea. *Deep Sea Res. Part II Top. Stud. Oceanogr.* **118**, 18–31 (2015).
34. M. Itoh *et al*., Water properties, heat and volume fluxes of Pacific water in Barrow Canyon during summer 2010. *Deep Sea Res. I Oceanogr. Res.* **102**, 43–54 (2015).
35. P. Winsor, D. C. Chapman, Pathways of Pacific water across the Chukchi Sea: A numerical model study. *J. Geophys. Res. Oceans* **109**, C03002 (2004).
36. Y.-C. Fang *et al*., Surface current patterns in the Northeastern Chukchi Sea and their response to wind forcing. *J. Geophys. Res. Oceans* **122**, 9530–9547 (2017).
37. R. S. Pickart *et al*., Upwelling in the Alaskan Beaufort Sea: Atmospheric forcing and local versus non-local response. *Prog. Oceanogr.* **88**, 78–100 (2011).
38. M. A. Spall, Circulation and water mass transformation in a model of the Chukchi Sea. *J. Geophys. Res.* **112**, C05025 (2007).
39. M. N. Pisareva *et al*., Flow of pacific water in the western Chukchi Sea: Results from the 2009 RUSALCA expedition. *Deep Sea Res I Oceanogr Res* **105**, 53–73 (2015).
40. C. J. Ashjian *et al*., Climate variability, oceanography, bowhead whale distribution, and Iñupiat subsistence whaling near Barrow, Alaska. *Arctic* **63**, 179–194 (2010).
41. M. A. Tyler, D. W. Coats, D. M. Anderson, Encystment in a dynamic environment: Deposition of dinoflagellate cysts by a frontal convergence. *Mar. Ecol. Prog. Ser.* **7**, 163–178 (1982).
42. D. M. Anderson *et al*., *Alexandrium fundyense* cysts in the Gulf of Maine: Long-term time series of abundance and distribution, and linkages to past and future blooms. *Deep Sea Res 2 Top Stud Oceanogr* **103**, 6–26 (2014).
43. D. J. McGillicuddy Jr *et al*., Suppression of the 2010 *Alexandrium fundyense* bloom by changes in physical, biological, and chemical properties of the Gulf of Maine. *Limnol. Oceanogr.* **56**, 2411–2426 (2011).
44. D. M. Anderson *et al*., Understanding interannual, decadal level variability in paralytic shellfish poisoning toxicity in the Gulf of Maine: The HAB Index. *Deep Sea Res 2 Top Stud Oceanogr* **103**, 264–276 (2014).
45. L. L. Bean, J. D. McGowan, J. W. Hurst, Annual variations of paralytic shellfish poisoning in Maine, USA 1997–2001. *Deep Sea Res. Part II Top. Stud. Oceanogr.* **52**, 2834–2842 (2005).
46. S. Shumway, S. Sherman-Caswell, J. W. Hurst, Paralytic shellfish poisoning in Maine: Monitoring a monster. *J. Shellfish Res.* **7**, 643–652 (1988).
47. D. M. Anderson *et al*., Initial observations of the 2005 *Alexandrium fundyense* bloom in southern New England: General patterns and mechanisms. *Deep Sea Res. Part II Top. Stud. Oceanogr.* **52**, 2856–2876 (2005).
48. M. L. Brosnahan, D. K. Ralston, A. D. Fischer, A. R. Solow, D. M. Anderson, Bloom termination of the toxic dinoflagellate *Alexandrium catenella*: Vertical migration behavior, sediment infiltration, and benthic cyst yield. *Limnol. Oceanogr.* **62**, 2829–2849 (2017).
49. M. Natsuike, H. Oikawa, K. Matsuno, A. Yamaguchi, I. Imai, The physiological adaptations and toxin profiles of the toxic *Alexandrium fundyense* on the eastern Bering Sea and Chukchi Sea shelves. *Harmful Algae* **63**, 13–22 (2017).
50. T. Y. Orlova *et al*., Morphogenetic and toxin composition variability of *Alexandrium tamarense* (Dinophyceae) from the east coast of Russia. *Phycologia* **46**, 534–548 (2007).
51. C. A. Stock, D. J. McGillicuddy, A. R. Solow, D. M. Anderson, Evaluating hypotheses for the initiation and development of *Alexandrium fundyense* blooms in the western Gulf of Maine using a coupled physical–biological model. *Deep Sea Res. Part II Top. Stud. Oceanogr.* **52**, 2715–2744 (2005).
52. C. J. Watras, S. W. Chisholm, D. M. Anderson, Regulation of growth in an estuarine clone of *Gonyaulax tamarensis Lebour*: Salinity-dependent temperature responses. *J. Exp. Mar. Biol. Ecol.* **62**, 25–37 (1982).
53. L. McRaven, R. Pickart, Conductivity-temperature-depth (CTD) data from the 2019 Distributed Biological Observatory - Northern Chukchi Integrated Study (DBO-NCIS) cruise on US Coast Guard Cutter (USCGC) Healy (HLY1901). Arctic Data Center. https://doi.org/10.18739/A2D21RK4M. Deposited 1 April 2021.
54. P. Wassmann *et al*., The contiguous domains of Arctic Ocean advection: Trails of life and death. *Prog. Oceanogr.* **139**, 42–65 (2015).
55. B. A. Keafer, K. O. Buesseler, D. M. Anderson, Burial of living dinoflagellate cysts in estuarine and nearshore sediments. *Mar. Micropaleontol.* **20**, 147–161 (1992).
56. A. Miyazono, S. Nagai, I. Kudo, K. Tanizawa, Viability of *Alexandrium tamarense* cysts in the sediment of Funka Bay, Hokkaido, Japan: Over a hundred year survival times for cysts. *Harmful Algae* **16**, 81–88 (2012).
57. L. McRaven, R. Pickart, Conductivity-temperature-depth (CTD) data from the 2018 Monitoring the Western Arctic Boundary Current in a Warming Climate: Atmospheric Forcing and Oceanographic Response (Arctic Observing Network) cruise on USCGC (US Coast Guard Cutter) Healy (HLY1803). Arctic Data Center. https://doi.org/10.18739/A28C9R51P. Deposited 1 April 2021.
58. L. McRaven, R. Pickart, Conductivity-temperature-depth (CTD) data from the 2018 Distributed Biological Observatory - Northern Chukchi Integrated Study (DBO-NCIS) cruise on USCGC (US Coast Guard Cutter) Healy (HLY1801). Arctic Data Center. https://doi.org/10.18739/A2HT2GC7Z. Deposited 1 April 2021.
59. A. R. Solow, A. R. Beet, B. A. Keafer, D. M. Anderson, Testing for simple structure in a spatial time series with an application to the distribution of *Alexandrium* resting cysts in the Gulf of Maine. *Mar. Ecol. Prog. Ser.* **501**, 291–296 (2014).
60. J. M. Grebmeier, Shifting patterns of life in the Pacific Arctic and sub-Arctic seas. *Annu. Rev. Mar. Sci.* **4**, 63–78 (2012).
61. D. M. Anderson *et al*., Identification and enumeration of *Alexandrium spp.* from the Gulf of Maine using molecular probes. *Deep Sea Res. Part II Top. Stud. Oceanogr.* **52**, 2467–2490 (2005).
62. R. E. Davis, Preliminary results from directly measuring middepth circulation in the tropical and South Pacific. *J. Geophys. Res. Oceans* **103**, 24619–24639 (1998).
63. K. Våge *et al*., Revised circulation scheme north of the Denmark Strait. *Deep Sea Res I Oceanogr Res* **79**, 20–39 (2013).
64. J. L. Smith, P. Wessel, Gridding with continuous curvature splines in tension. *Geophysics* **55**, 293–305 (1990).
65. M. Yamaguchi, S. Itakura, I. Imai, Y. Ishida, A rapid and precise technique for enumeration of resting cysts of *Alexandrium spp.* (Dinophyceae) in natural sediments. *Phycologia* **34**, 207–214 (1995).
66. E. L. Lilly, K. M. Halanych, D. M. Anderson, Species boundaries and global biogeography of the *Alexandrium tamarense* complex (Dinophyceae)1. *J. Phycol.* **43**, 1329–1338 (2007).
67. U. John *et al*., Formal revision of the *Alexandrium tamarense* species complex (Dinophyceae) taxonomy: The introduction of five species with emphasis on molecular-based (rDNA) classification. *Protist* **165**, 779–804 (2014).
68. W. F. Prud'homme van Reine, Report of the nomenclature committee for algae 15. *Taxon* **66**, 191–192 (2017).
69. W. B. Corlett, R. S. Pickart, The Chukchi slope current. *Prog. Oceanogr.* **153**, 50–65 (2017).